Unravelling discharge and surface mechanisms in plasma assisted ammonia reactions

Paula Navascués,[a] Jose M. Obrero-Pérez,[a] José Cotrino,[a,b] Agustín R. González-Elipe*[a] and Ana Gómez-Ramírez*[a,b]

[a] Laboratory of Nanotechnology on Surfaces and Plasma. Instituto de Ciencia de Materiales de Sevilla (CSIC-Universidad de Sevilla), Avda. Américo Vespucio 49, E-41092 Seville, Spain.

[b] Departamento de Física Atómica, Molecular y Nuclear, Universidad de Sevilla, Avda. Reina Mercedes, E-41012 Seville, Spain

* Corresponding authors

anamgr@us.es

arge@icmse.csic.es

Abstract. Current studies on ammonia synthesis by means of atmospheric pressure plasmas respond to the urgent needs of developing less environmentally aggressive processes than the conventional Haber-Bosch catalytic reaction. Herein, we systematically study the plasma synthesis of ammonia and the much less investigated reverse reaction (decomposition of ammonia into nitrogen and hydrogen). Besides analyzing the efficiency of both processes in a packed-bed plasma reactor we apply an isotope exchange approach (using D_2 instead of H_2) to study the reaction mechanisms. Isotope labelling has been rarely applied to investigate atmospheric plasma reactions and we demonstrate for the first time that this methodology may provide unique information about intermediate reactions that, consuming energy and diminishing the process efficiency, do not effectively contribute to the overall synthesis/decomposition of ammonia. In addition, same methodology has demonstrated the active participation of the interelectrode material surface in the plasma-activated synthesis/decomposition of ammonia. These unprecedented results about the involvement of surface reactions in packed-bed plasma processes, complemented with data obtained by optical emission spectroscopy of the plasma phase, have permitted to unravel key mechanisms of the ammonia synthesis/decomposition reactions in packed-bed reactors and to propose a general strategy to increase the yield and energy efficiency of these processes.

Keywords: packed-bed plasma reactors, ammonia synthesis, hydrogen production, atmospheric pressure plasma, energy efficiency, inefficient plasma processes, ferroelectric materials.

INTRODUCTION

During the last years plasma and plasma-catalysis reactions carried out in packed-bed plasma and other type of atmospheric pressure reactors have emerged as a suitable technology to promote different gas phase processes of high environmental impact. Examples encompass the removal of contaminants,[1–6] the methane, hydrocarbons and alcohols reforming[7–12] or the ammonia synthesis.[13–15] Advantages of plasma and plasma-catalysis for these applications are their low temperature of operation, the possibility to work at atmospheric pressure or bellow, its straightforward down-scaling

to small reactor sizes or the null induction period required to achieve steady state conditions, all together enabling a distributed application of the technology directly connected to the grid.[16] However, these good prospects have stubbornly confronted serious and up no to now unsolved limitations such as a poor energy efficiency and a low selectivity for the synthesis of given compounds. Different atmospheric plasma processes (e.g. gliding arcs or dielectric barrier discharges) and reactor designs[17–23] or the use of different kind of moderator materials for packed-bed discharges (e.g., ferroelectrics instead of dielectrics)[24–26] have been proposed to overcome energy efficiency limitations. Conventional and novel (e.g. mesoporous or nanoparticles) catalysts have been incorporated together with the dielectric material in the inter-electrode space of packed-bed reactors to improve selectivity and energy efficiency.[20,21,26–31] Herein we will show that, in addition to engineering improvements, overcoming energy/selectivity bottlenecks require new basic knowledge about the mechanisms of these atmospheric pressure plasma processes.

The present work is primarily driven by the need of improving the performance of the plasma synthesis of ammonia in a scenario where, at global scale, the catalytic Haber-Bosch process is responsible for ca. 1.2% of the global CO_2 emissions.[16] The requisite of combining the reduction of energy consumption with the production of ammonia in a distributed way close to final users has called for an active investigation of a variety or alternative processes, including plasma-catalysis.[13–22,24–39] A second motivation of this work is the use of ammonia as suitable hydrogen storage vector and the advantages, with respect to classical catalysis,[40–42] of small plasma reactors for its low temperature decomposition into hydrogen, as required for mobile device applications.

Although a remarkable 7% reaction yield has been reported for the plasma synthesis of ammonia at atmospheric pressure and ambient temperature,[25] this value is still far from the 10-15% yield of the catalytic Haber-Bosch process. In addition, this plasma reaction yield is further jeopardized by its comparatively low energy efficiency. Trying to approach this problem from a new perspective, the present investigation proposes to study at fundamental level the ammonia synthesis/decomposition reactions evaluating the extent of intermediate plasma processes which, consuming energy, do not contribute to increase the yield of final products. Such a conceptual approach has not been systematically applied in the field of atmospheric plasmas, even though it would provide critical knowledge for a scientifically founded design of reactors and the definition of better reaction operational conditions. For this endeavor, we propose an isotope labelling methodology which, being rather common in conventional catalysis, has been scarcely utilized in plasma-catalysis.[7,35,43] In particular, we have investigated the isotopic exchange for mixtures NH_3+D_2 and NH_3+N_2+D_2 to determine the extent by which the back decomposition reaction (i.e., $2NH_3 \rightarrow N_2 + 3H_2$, note that increasing the performance of this reaction is of interest from the viewpoint of hydrogen storage applications) and other inefficient hydrogen exchange processes detract plasma

energy and contribute to lower the efficiencies of current processes for the plasma synthesis of ammonia. In the curse of these investigations, we have also realized that isotope labelling may also provide information about intermediate processes that, having been accepted to occur in plasma-catalysis reactions, have not been experimentally tested. We refer to the direct involvement of the surface of the moderator and/or catalyst in the reaction mechanisms. With this purpose we have studied the N_2+D_2 and N_2+H_2 plasma reactions, the latter after prolonged exposure of the inter-electrode material (i.e., lead zirconate titanate – PZT – in our case) to a D_2 plasma, and followed the H/D isotope distribution in the produced ammonia. Overall, the isotope exchange results, together with the analysis of the optical emission spectra of the plasmas, have permitted to unravel basic mechanisms and the role of intermediate plasma species in the plasma synthesis/decomposition of ammonia. The understanding gained about these basic mechanisms has also served to propose possible solutions to overcome current limitations in the design and functioning of packed-bed plasma reactors.

EXPERIMENTAL SECTION

Packed-bed reactor and operating conditions

Experiments were carried out in a packed-bed reactor operated at atmospheric pressure that has been described in detail elsewhere.[24,25,35] It mainly consists of a ferroelectric packed-bed of lead zirconate titanate (PZT) pellets placed between two parallel plate stainless steel electrodes (75 mm in diameter). The upper electrode was connected to a high voltage power amplifier (Trek Inc., USA, Model PD05034), coupled to an AC function generator (Stanford Research Systems, USA, Model DS345), while the bottom electrode was grounded. More detailed information about the reactor set-up and its operation can be found in Supporting Information 1. AC voltage amplitude varied between 2 and 4 kV at a frequency of 5 kHz, if not otherwise stated. Electrical characterization of the discharge was made by means of an oscilloscope (Agilent Tech., USA, Model DSO-X 3924A) directly connected to a high voltage probe (to acquire V(t)) and a series resistance (to acquire I(t)). The average power consumed in the process (P) was determined by the area of the Lissajous plot recorded for each experiment[44] (see Supporting Information 2 for a more detailed description).

All gases utilized, N_2, D_2, H_2 and NH_3, were supplied by Air Liquide (Alphagaz, Spain). Molecules, compounds and molecular fragments will be designated with their formulas, taking into account the presence of either H or D atoms in their structure (e.g., HD, ND_2H, etc.). However, the terms *hydrogen* and *ammonia* in cursive script will be used when referring to the complete set of labelled molecules of each specific compound.

To evaluate the effect of residence time on reaction mechanisms, we varied the total gas flow rate of reactants, but always keeping the same proportion between gas

mixture components. Values of reactant gas flow rates are given in the text. Although all experiments were performed at ambient temperature, a small thermal drift in temperature up to 40ºC at the reactor walls occurred after long operating periods.

Gas and isotope exchange monitoring

To analyse the composition of reactor outlet mixtures and to follow isotopic exchange processes we used a Quadrupole Mass Spectrometer (Pfeiffer Vacuum, Germany, QMG 220 Prisma Plus). A typical example of the spectrometer response when analysing isotope exchange processes involved in the ammonia synthesis/decomposition reactions can be seen in Supporting Information 3. From the intensity of the different *m/z* peaks attributed to either *hydrogen* (i.e., H_2, HD, D_2) or *ammonia* (i.e, NH_3, NDH_2, ND_2H and ND_3) species it is possible to quantitatively determine the percentage of labelled molecules in each product and its evolution with the utilized experimental conditions (see a previous work[35] and the Supporting Information 3).

Occasionally, mass spectrometry analysis was complemented by results obtained with an infrared (FT-IR) spectrometer (Agilent Technology, USA, Cary 630 FTIR) located in series with the reactor and before the quadrupole. The spectra were registered with a resolution of 1 cm^{-1}. Results by this technique that complement those obtained by mass spectrometry will be reported only for some of the experiments.

Optical Emission Spectroscopy (OES) was used for in situ plasma diagnosis. The spectra were measured by a monochromator (Horiba Ltd., Japan, Jobin-Yvon FHR640), with a resolution of 0.1 nm. An optical fibre feed-trough was situated in the lateral wall of the reactor to collect the light emitted by the plasma (see Supporting Information 1).

Reaction yield and energy efficiency

For the ammonia synthesis reaction, the so-called chemical yield, Y_{N2} (%), and the energy efficiency for the production of ammonia, EE-NH_3 (gNH_3/kWh) are defined as:

$$Y_{N_2} = \frac{M_{NH_3}(out)}{2 \cdot \mathrm{M}_{N_2}(in)} \cdot 100 \qquad (E1)$$

$$EE - NH_3 = \frac{m_{NH_3}(out) \cdot 60}{P} \qquad (E2)$$

where M_{NH3}(out) and M_{N2}(in) refer to the flows of these gases in the product and reactant mixtures, respectively, m_{NH3}(out) is the amount of produced ammonia (in grams) and P is the average power consumed in the process.

For the ammonia decomposition reaction, the decomposition yield, DY_{NH3} (%) and the energy efficiency for H_2 production, EE-H_2 (LH_2/kWh) are defined as:

$$DY_{NH_3} = \frac{\mathrm{M}_{NH_3}(in) - \mathrm{M}_{NH_3}(out)}{\mathrm{M}_{NH_3}(in)} \cdot 100 \qquad (E3)$$

$$EE - H_2 = \frac{V_{H_2}(out) \cdot 60}{P} \qquad (E4)$$

where V_{H2}(out) refers to the volume (in liters) of H_2 produced by the decomposition of ammonia, i.e., discarding hydrogen in the reactant mixture.

Inefficient reaction events

The concept of inefficient *reaction event*, defined in previous work,[35] designates the occurrence of intermediate processes that are ineffective in producing a valuable "product" molecule (either *ammonia* or *hydrogen* depending on the intended process). Examples illustrating this type of inefficient intermediate *events* for *ammonia* production are provided in Supporting Information 4

The minimum number of inefficient *reaction events* (RE) associated to the formation of ND_2H molecules is defined as:

$$RE_{\mathrm{NHD}_2} = (\%ND_2\mathrm{H} \cdot 2) \cdot \frac{M_{NH_3}(out)}{Total\ flow\ (out)} \qquad (E5)$$

where $\%ND_2H$ refers to the percentage of this molecule within the *ammonia* molecules and the multiplying factor 2 refers that this molecule requires at least two intermediate reactions to be formed in a mixture of D_2 plus NH_3. Similar definitions can be made for NDH_2 or ND_3 and for the minimum number of inefficient events associated to the formation of *ammonia*:

$$RE_{Amm.} = (\%NDH_2 \cdot 1 + \ \%ND_2\mathrm{H} \ \cdot 2 + \%ND_3 \cdot 3) \cdot \frac{M_{NH_3}(out)}{Total\ flow\ (out)} \qquad (E6)$$

A similar definition can be made for the various forms of labelled *hydrogen* (i.e., H_2 and HD if using D_2 as reactant) and for the minimum total number of inefficient reaction events (TRE):

$$TRE = RE_{Ammonia} + \ RE_{Hydrogen} \qquad (E7)$$

RESULTS AND DISCUSSION

Ammonia decomposition reactions

In previous works we have shown that, a mixture of nitrogen and hydrogen fed in the appropriate concentrations into a packed-bed reactor produces a certain amount of ammonia. This could be maximized up to 7% of nitrogen conversion by properly adjusting the N_2:H_2 ratio, the operating electrical parameters, the size and type of interelectrode material, the distance between electrodes and the residence time of gases.[24,25] These results proved that residence time of reactants is a critical parameter to control efficiency, although no linear relationship exists between this parameter and

production of ammonia. This deviation from linearity suggested that besides the ammonia synthesis reaction, there are other plasma processes that are inefficient to produce ammonia. One of these reaction processes might be the *partial decomposition of the formed ammonia into nitrogen and hydrogen.*

If ammonia decomposes into N_2 and H_2, this process will reduce the ammonia synthesis rate and the energy efficiency for the ammonia synthesis process. However, maximizing the decomposition yield would be aimed when hydrogen is the desired product of ammonia decomposition. Pure ammonia decomposition results are shown in Figure 1 and Table 1. Data in this figure show that more than 30% ammonia decomposed in this experiment and that decomposition yield only decreased by 7-8% for a three times higher flow. It is noteworthy that energy efficiency in this hydrogen production experiment is similar to that previously reported for the wet reforming of methane in the same reactor.[45]

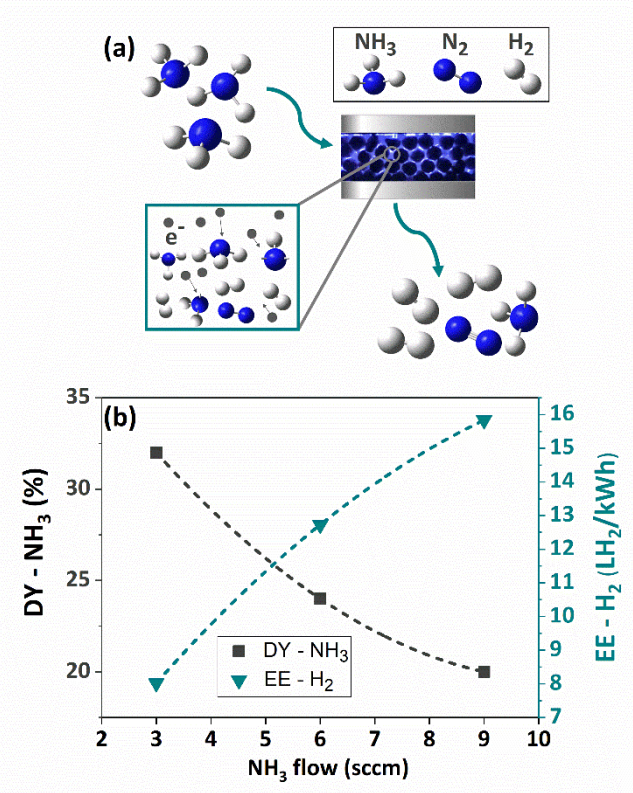

Figure 1. (a) Scheme of the ammonia decomposition reaction indicating that three H_2 and one N_2 molecules are formed from the decomposition of two ammonia molecules due to plasma processes triggered by the interaction with plasma electrons (see the square inset for illustration). (b) Plots of NH_3 decomposition yield and Energy Efficiency for H_2 production represented against NH_3 flow, varying from 3 to 9 sccm. The experiment was carried out at a frequency of 5 kHz and a voltage amplitude of 2 kV (consumed power 10 ± 1 W).

The relatively high-energy efficiency of the ammonia plasma decomposition reaction supports a high reversibility for the process: $N_2 + H_2 \Leftrightarrow NH_3$. This assessment was further confirmed by the decomposition yields and energy efficiencies found in

experiments reported in Table 1 for mixtures NH_3+N_2 and NH_3+H_2 (total flow 9 sccm). Since values of these two parameters were similar for pure NH_3 and a mixture NH_3+N_2 (ratio 1:2), we can conclude that plasma electrons preferentially activate ammonia over nitrogen molecules. For the mixture NH_3+H_2, however, experiment revealed a net loss of energy efficiency, suggesting that hydrogen competes more efficiently than nitrogen (and as efficiently as ammonia) for the plasma electrons. This inference agrees with that H_2 has a higher electron impact ionization cross section than N_2 (e.g., for 16 eV electrons values are 0.013 $Å^2$ and 0.034 $Å^2$ for N_2 and H_2, respectively).[46] This experiments also suggests that hydrogen radicals or excited species may recombine or become exchanged with hydrogen atoms in ammonia molecules or fragments with null decomposition of this compound (i.e., what we call *inefficient reaction events*). In next sections, using the isotope labelling technique with mixtures NH_3+D_2 and NH_3+D_2+N_2, we will study these exchange reactions.

Table 1. Ammonia decomposition. Decomposition yield of ammonia and energy efficiency associated to H_2 production for a plasma of NH_3 and mixtures of this gas with N_2 or H_2 (current amplitude was fixed constant at 25 mA).

Gas or mixture	Total flow rate (sccm)	DY-NH_3 (%)	EE-H_2 (LH_2/kWh)
NH_3	3	32	8.0
	6	24	13
	9	20	16
NH_3 + N_2	9 (ratio 1:2)	19	16
NH_3 + H_2	9 (ratio 2:3)	17	6.0

Ammonia decomposition vs. isotope exchange reactions

The reversibility between ammonia synthesis and decomposition reactions strongly suggests the occurrence of hydrogen atom exchanges between ammonia and hydrogen molecules, as well as other intermediate processes. Experiments utilizing a NH_3+D_2 reactants mixture (NH_3:D_2 ratio of 2:3) provided interesting clues to account for the nature and extent of these intermediate processes. A summary of the results obtained is reported in Figure **2**. Figure **2(a)** shows a clear evolution in the intensity of the recorded *m/z* peaks as a function of power (i.e., basically a progressive decrease in the intensity of peaks associated to D_2 and NH_3 and an increase of those due to H_2, HD, NDH_2 and ND_2H (c.f., Figure **2**)). As illustrated by the schemes in Figure **2(b),** this evolution sustains that a series of isotopic exchange processes of the type:

$$NH_3 + D_2 \rightarrow ND_XH_Y + HD\ (H_2) \quad (E8)$$

progressively increased with the plasma power.

From the analysis of the intensity of the different *m/z* peaks (see Supporting Information 3), it is possible to estimate the partition of the difference labelled molecules in a given compound (i.e., H_2, HD and D_2 for *hydrogen* and NH_3, NDH_2, ND_2H and ND_3 for *ammonia*). The histogram plots in Figures **2(c)** and **2(d)** represent the

percentages of the different labelled molecules as a function of plasma power for a fixed flow of reactants (9 sccm), or as a function of the total flow of reactants at constant power (9 ± 1 W).

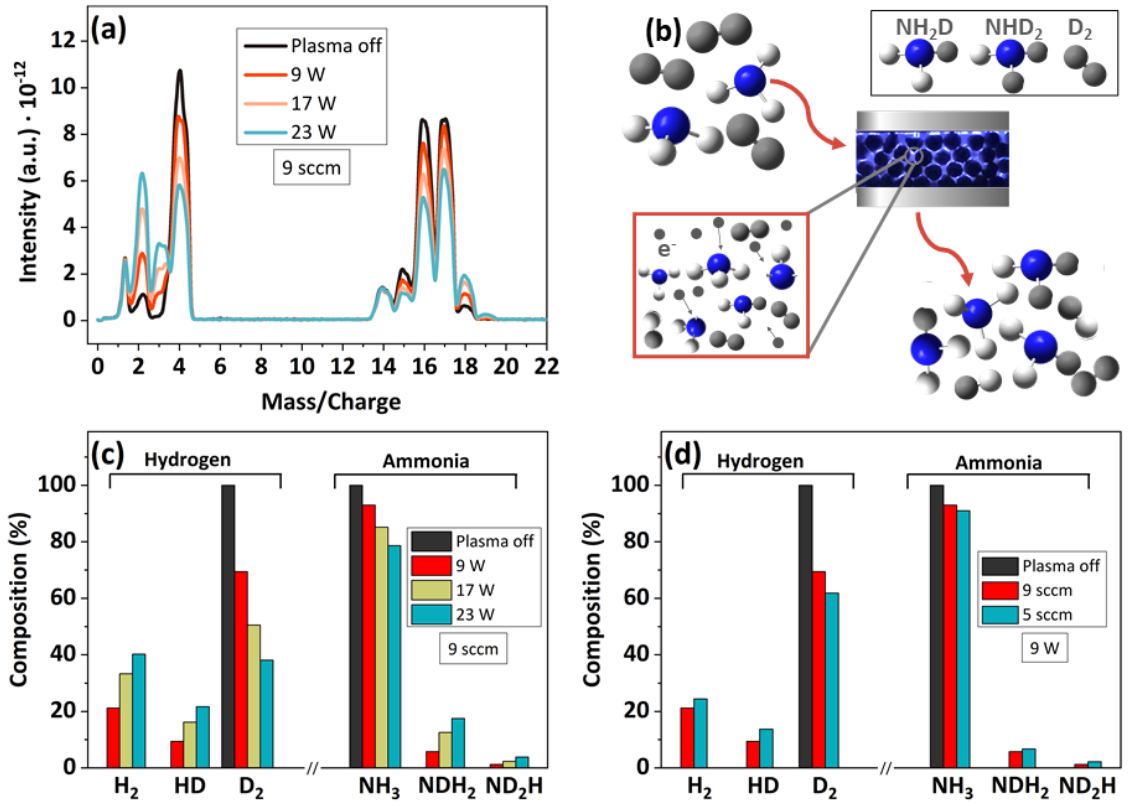

Figure 2. (a) Series of mass spectra recorded for plasma activated NH_3+D_2 mixtures at increasing powers from 9 to 23 W (total flow fixed at 9 sccm). (b) Scheme showing the plasma exchange processes leading to the formation of ammonia and hydrogen molecules labelled with deuterium. (c) Histogram from (a), showing the percentage of the different deuterium and ammonia labelled molecules as a function of plasma power. (d) Idem as a function of total flow (power fixed at 9 ± 1 W). The experiments were carried out at a frequency of 5 kHz and a variable voltage amplitude from 2.5 to 4 kV.

A first evidence regarding these column plots is that NH_3 and D_2 progressively decrease in the outlet gas mixture because they progressively exchange their constituent H/D atoms according to processes such as those represented in (**E8**). According to Figures **2(c)** and **(d)** these exchange reactions are more frequent when increasing power and residence time (i.e., decreasing the reactant flow) and may produce up to 60% reduction of D_2 molecules in the total amount of *hydrogen* in the outlet mixture. In next sections, analyzing the evolution of ternary N_2+D_2+NH_3 mixtures, we will show that plasma energy may induce exchange processes and no net synthesis/decomposition of ammonia.

In the present experiment with NH_3+D_2 we found a little but progressive increase with power in the *m/z=28* peak intensity (see Supporting Information 5). This evidence, joined to the observed decrease in the amount of *ammonia* molecules between inlet and outlet flows proved that a fraction of ammonia was effectively decomposed into nitrogen and hydrogen. Table **2** summarizes the results for various experimental conditions. Data include the NH_3 decomposition yield (i.e., according to **(E3)**) and the partition between the decomposed NH_3 molecules leading to N_2 (and *hydrogen*) and the NH_3 molecules that have exchanged H by D. In other words, this partition quantifies the ammonia molecules decomposed into *hydrogen* and N_2 (fourth column) or those that have undergone H by D exchange (fifth column).

Table 2. Evolution of the decomposition yield of ammonia and estimation of fractions of ammonia decomposed molecules and H--D exchange processes as a function of ammonia flow rate and plasma power

NH_3 flow rate (sccm)	**Power (±1 W)**	**DY-NH_3 (%)**	**Fraction of decomposed NH_3 molecules**	**Fraction of reacting NH_3 molecules that have exchanged H by D**
9	9	0.24	0.03	0.97
	17	8.9	0.40	0.60
	23	17	0.49	0.51
5	9	12	0.47	0.53
3	5	11	0.58	0.42

Moreover, this table shows that both ammonia decomposition yield and fraction of NH_3 molecules decomposed into N_2 and *hydrogen* (HD may be formed through secondary processes) increase with power and residence time, while the fraction of ammonia molecules that undergo inefficient H--D exchanges follows an opposite behavior. From a practical point of view, these opposed tendencies show that *operating packed-bed plasmas at high input powers favor the decomposition of the ammonia into hydrogen and nitrogen with respect to hydrogen exchange reactions.*

Isotopic exchange events under steady state conditions

Mixtures Nitrogen + Hydrogen + Ammonia represent the typical composition of outlet gases during ammonia synthesis/decomposition experiments. To quantitatively estimate to which extent hydrogen exchange and similar intermediate processes waste energy without contributing to the formation/decomposition of ammonia we studied a ternary inlet mixture N_2+D_2+NH_3 with adjusted molecular ratios such that no net formation/depletion of nitrogen occurs after plasma ignition, i.e., the inlet ratio N_2/NH_3 is the same than the outlet ratio $N_2/(NH_3$+ NDH_2+ND_2H+$ND_3)$. Such conditions were found for inlet mixtures with a N_2:D_2 constant ratio of 1:3, a NH_3 constant flow of 3.7 sccm and total flows of 15, 27 and 38 sccm.

The bar diagrams in Figure 3 show the partitions of the different labelled molecules in each compound (i.e. *hydrogen* or *ammonia*), either as a function of the power or for

three total flows of reactants. These latter conditions were selected to check the influence of residence time in the exchange processes. The diagrams indicate that the relative concentrations of NDH_2 and ND_2H, as well as hints of ND_3, increase with the applied power (Figure 3(a)) and for smaller flow rates (Figure 3(b)). A similar tendency was found for the evolution of H_2 and HD molecules.

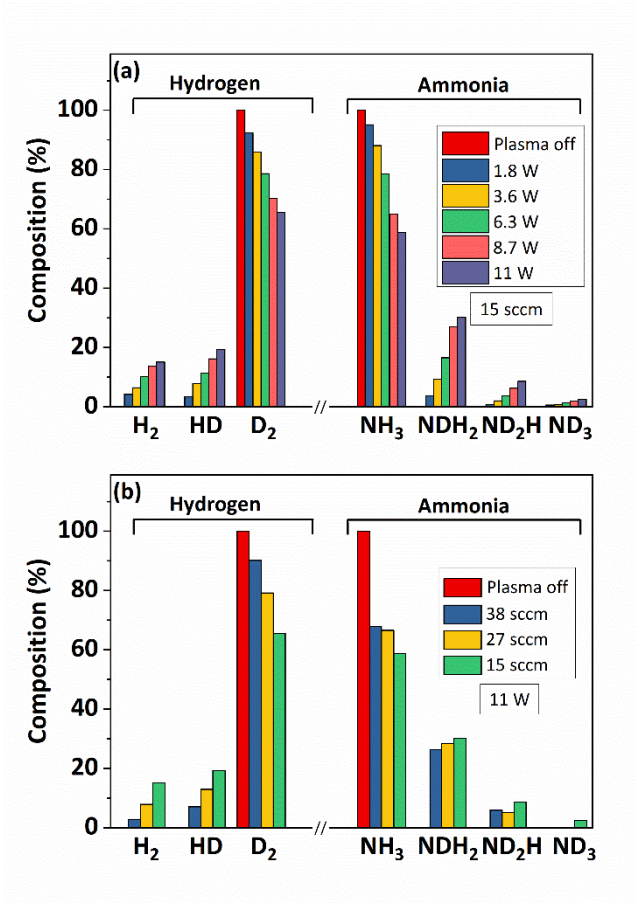

Figure 3. Percentages of the different labelled molecules in *hydrogen* and *ammonia* detected for the ternary reactants mixture NH_3+D_2+N_2 as a function of (a) the applied power (for V=2.5 kV, flow rate of 15 sccm and frequency between 1 and 5 kHz) and (b) the total input flow of reactants (i.e., 38, 27 and 15 sccm) for a power of 11 W (2.5 kV, 5 kHz).

These results confirm that, under the investigated conditions, H--D exchange reactions are massively taken place with zero energetic efficiency for the production/decomposition of ammonia.

To more precisely assess how plasma energy is consumed in promoting plasma exchange reactions we apply the *reaction events* concept proposed in the experimental section. Figure 4 shows representations of the evolution of the number of *events* for *ammonia* and *hydrogen* as a function of the total flow rate for an applied power of 11 W (same conditions than for the histogram in Figure **3(b)**). In these plots, overall data are also provided for *hydrogen* (i.e., sum of events associated to HD and

H_2), *ammonia* (i.e., sum of events associated to NDH_2, ND_2H and ND_3) and the sum of these two (TRE, see (**E-7**)). Clearly, there is a progressive decrease in the number of *events* when the total flow rate increases (i.e. residence time decreases). Similarly, a progressive increase in the number of *events* was found when increasing the plasma *power* (see Supporting Information 6 showing the *reaction events* dependence on power). Interestingly, Figure 4 also shows that hydrogen is more likely to undergo exchange *events* than ammonia. From a practical point of view, this *evidence suggests that a suitable strategy to increase the energy efficiency for the synthesis of ammonia would consist of properly adjusting the hydrogen flow, while if the objective is to decompose ammonia, produced hydrogen should be removed from reaction medium immediately after its formation* (e.g., using selective diffusion membranes).[47]

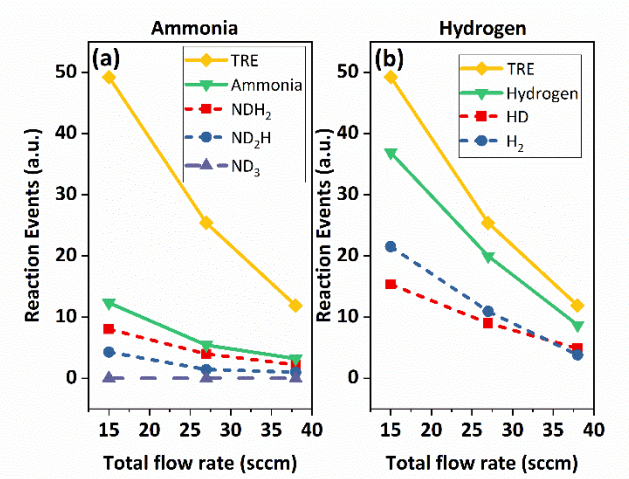

Figure 4. Representation of the number of *events* for (a) ammonia and (b) hydrogen molecules detected in the outlet mixture during the analysis of the stationary mixture NH_3+D_2+N_2 as a function of total flow rate (applied power of 11 ± 1W).

Intermediate plasma species during plasma synthesis/decomposition of ammonia

The isotopic exchange reactions must involve different excited plasma species. Typical OES spectra as a function of power for the NH_3+D_2 mixture above are shown in Figure **5(a),** where the emission lines can be attributed to N_2* and NH* (ND*) species.[48] This assignment relies on similar plasma investigations where peaks between 290-385 nm were attributed to the second positive system of N_2* species $[C^3\Pi \rightarrow B^3\Pi]$, and the peak at 336 nm to NH* species.[24,25] Interestingly, unlike the spectra recorded for mixtures N_2+H_2,[24,25] only hints of a peak at 391.4 nm usually attributed to N_2^+ species $[B^2\Sigma_u^+ \rightarrow X^2\Sigma_g^+]$ can be detected in the spectrum taken at maximum power. Also, a slightly increase in the spectral background at lower wavelengths observed in this high power spectrum can be related with the presence of excited deuterium (hydrogen)

species in the plasma gas (see the background in Figure **5(a)** at 23 W and Supporting Information 7).[49]

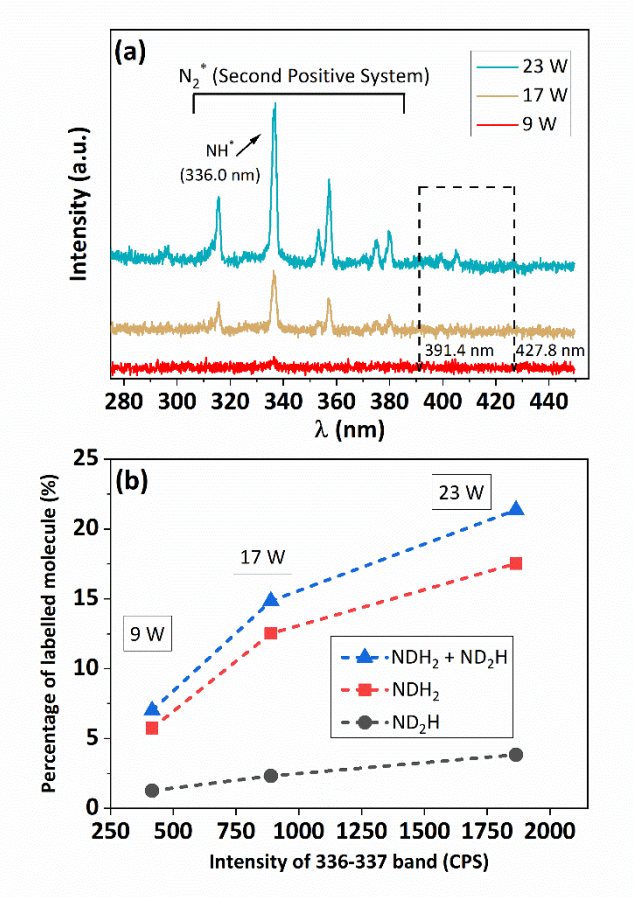

Figure 5. (a) Series of OES recorded for a NH_3+D_2 plasma mixture (9 sccm) as a function of the applied power. (b) Plot of the percentage of ammonia molecules containing deuterium (data taken from Figure 3(c)) against the intensity of the 336-337 band (associated to NH*) for the indicated applied power.

The progressive formation of NH* (ND*) species as the power increases and its correlation with the percentage of labelled molecules NDH_2 and ND_2H (c.f., Figure 3(b)) suggest that D exchange reactions are involved in the formation of NH* (ND*) and NH_2* (ND_2* or NDH*) intermediate radicals via processes E9-E13**:** [13]

$$NH_3 + e^- \rightarrow NH^* + 2H^* \quad (E9)$$

$$NH_3 + e^- \rightarrow NH_2^* + H^* \quad (E10)$$

Once NH* and NH_2* radicals are formed it is likely their interaction with D_2 according to:

$$NH^* + D_2 \rightarrow NDH^* + D^* \quad (E11)$$

$$NH_2^* + D_2 \rightarrow NDH_2 + D^* \quad (E12)$$

or, in a second step:

$$NDH^* + D_2 \rightarrow ND_2H + D^* \quad (E13)$$

Since OES detects line emissions from NH*(ND*) but not from NH_2^* (ND_2*, NDH*), this suggests a higher reactivity and a shorter life time for NH_2* species; in other words, that reactions (E10, E12 and E13) are very fast and drastically contribute to lower or remove these intermediate species from the plasma. Previous investigations in other type of plasmas as inductively coupled radiofrequency discharges[50] or plasma jets, [51] also support a higher stability of NH* species.

In addition, D* radicals formed by electron impact dissociation:

$$D_2 + e^- \rightarrow 2\ D^* \quad (E14)$$

are expected to react with NH_3 (NDH_2, ND_2H) molecules and contribute to isotopic exchange processes such as:

$$NH_3 + D^* \rightarrow NDH_2 + H^* \quad (E15)$$

The drift in the spectral background in Figure **5(a)** is an indirect evidence of deuterium (hydrogen) radicals formation.[49] In this figure, it is noteworthy the absence of spectral features around 391.4 and 427.8 nm due to N_2^+ species. The formation of this molecular ion has been reported in previous works dedicated to synthesis of ammonia in nitrogen rich conditions.[24,25] Their absence in Figure **5** is due to the small concentration of nitrogen formed and the aforementioned low electron impact ionization cross section of N_2.[46]

Surface vs. plasma intermediate reactions

A key feature in plasma and plasma catalysis reactions is to determine the involvement of plasma-surface processes. Although evidences of surface activated processes exist for low pressure plasmas[52] and are a common assumption in plasma-catalysis,[53,54] there are few direct experimental evidences confirming that plasma-surface processes participate in the reaction.[36] Herein, we have proved that surface processes actively participate in the ammonia synthesis and decomposition reactions.

In a first experiment, using a mixture N_2+D_2 (flow ratio 1:3), we found that besides the expected ND_3 molecules (i.e. equivalent to NH_3), labeled molecules such as NH_3, NDH_2 and ND_2H (together with HD) were detected by mass spectrometry and FT-IR analysis in the outlet flow. The series of mass spectra in Figure **6(a)** taken before and after igniting the plasma (5kHz; 3.5 and 4 kV) clearly show the formation of these labelled molecules. Analogously, the FT-IR spectra in Figure **6(b)** shows the appearance of bands at 2420, 2505 and 2558 cm^{-1}, attributed to labelled species of ammonia[55–57] and whose intensity increases with the applied power.

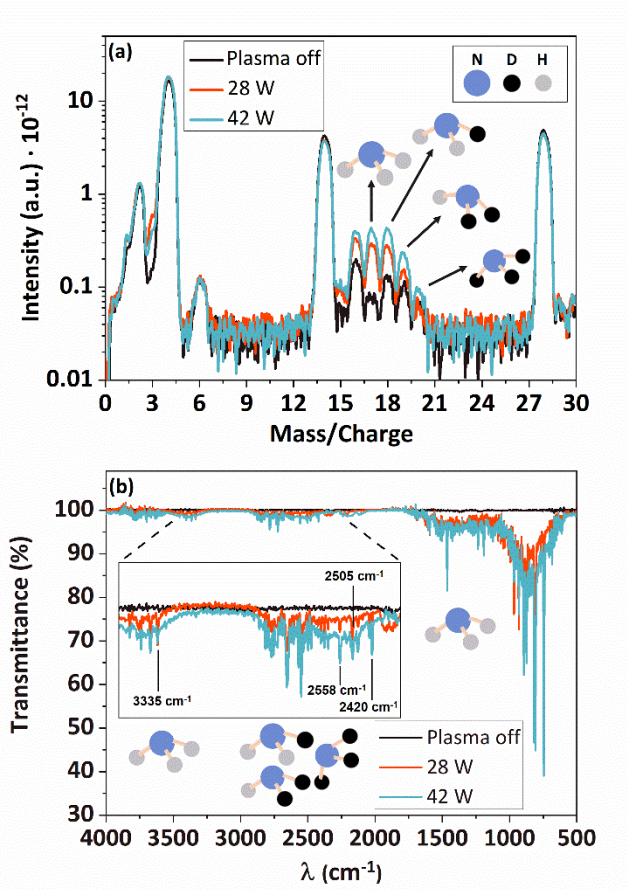

Figure 6. (a) QMS spectra taken at increasing powers (total flow rate 12 sccm). (b) Idem, FT-IR spectra of the outlet gas flow recorded simultaneously. The experiments were carried out at a frequency of 5 kHz and voltage amplitudes of 3.5 and 4 kV.

In this experiment, we also found that the partition of labelled molecules changed with the total flow of gases (c.f., Table 3). For the lowest flow the concentration of H containing molecules was higher, showing that H isotopes from an unknown source inside the reactor intervene in the *ammonia* synthesis reaction. We propose that these H atoms proceed from the surface and bulk of ferroelectric pellets placed in the inter-electrode space.

Table 3. Percentages of the different ammonia deuterium-labelled molecules detected one hour after igniting the plasma (applied power of 42 W) for experiments carried out for two input flow rates of N_2+ D_2.

Total flow rate of N_2+D_2	**12 sccm**	**34 sccm**
Molecular Specie	Relative (%)	Relative (%)
ND_3	7	60
ND_2H	22	28
NDH_2	42	1
NH_3	29	11

Another experiment complementing the previous one was carried out as follows. First, the ferroelectric pellets were exposed for 3 hours to a deuterium plasma (1.5 sccm of

pure D_2 at 4 kHz and 3.7 kV). During this pre-treatment mass spectrometry analysis showed the formation of HD molecules (see Supporting Information 8), indicating the existence of a H--D exchange process when PZT pellets were exposed to a plasma of pure D_2. This experiment also suggested that there were H atoms incorporated in the pellets before plasma ignition. The experiment continued with the ignition of a plasma of 3 sccm of N_2, followed by that of a N_2+H_2 mixture. Supporting information S9 (figure S9(a)) shows that no traces of either HD or D_2 molecules were detected when exposing the D_2 plasma treated PZT pellets to a N_2 plasma.

However, when shortly thereafter a N_2+H_2 plasma was ignited again (total flow rate of 34 sccm; 5 kHz, 3.3 and 4.1 kV), NDH_2, and ND_2H molecules were detected by mass spectroscopy (see Figure S9(b) in Supporting information S9). These findings confirm the involvement of deuterium, likely incorporated in the ferroelectric pellets, in the generation D-labelled ammonia molecules and suggest that i) a source of hydrogen exists in the PZT pellets used for plasma ammonia reactions, ii) this hydrogen can be mobilized when the pellets are exposed to a plasma containing H_2 or D_2 and iii) H/D exchange reactions involving ammonia molecules may take place for N_2 +H_2(D_2) plasmas.

A condition enabling these three working hypotheses is the incorporation of deuterium/hydrogen into the PZT pellets when they are exposed to a plasma containing hydrogen. Under these conditions the direct interaction of PZT with H*(D*) radicals and, possibly, other excited species of hydrogen, should promote the incorporation of H(D) onto the surface and likely also the interior of the PZT pellets. Large amounts of atomic hydrogen incorporation is known to occur in PZT treated either thermally with hydrogen or activated electrochemically with a Pt electrode in a water solution.[58,59] Similarly to the incorporation of hydrogen atoms in these experiments, we assume that activated hydrogen (deuterium) plasma atoms will readily interact with PZT and become incorporated both onto its surface and in its bulk. According to different works in literature, the capacity of PZT to incorporate hydrogen is very high and can amount to one atom per structural octahedral unit of its structure (maximum 1H:1Pb ratio).[60,61]

Therefore, assuming the availability of H(D) atoms incorporated in the PZT after hydrogen plasma activation (see Supporting Information S10 for a rough estimate of H/D incorporated in the pellets), we propose that surface reaction processes of the type E16-E18 take place during ammonia synthesis/decomposition reactions (equations written for the N_2+D_2 experiment):

$$ND^* (plasma) + -H (surf.) \rightarrow NH^* (plasma) + -D (surf.) \quad (E16)$$

$$ND^* (plasma) + -H (surf.) \rightarrow NDH^* (plasma) \quad (E17)$$

$$NDH^* (plasma) + -H(surf.) \rightarrow NDH_2 (gas) \quad (E18)$$

Where long living ND* species interact with the surface and may take or exchange D by H atoms from the PZT. Note that formation of NH* species by direct interaction of long living N_2* or N_2^+ plasma species with PZT must be discarded because no ammonia was detected when pellets were exposed to a plasma of pure nitrogen (see Supporting Information S9(a)).

In summary, based on the OES spectra and deuterium exchange reactions, we propose that, in the plasma phase, the most active (and short living) NH_2* radical participates actively in the plasma synthesis/decomposition of ammonia (and laterally in H(D) exchange processes). In addition, we also propose that the interaction of longer living ND* species and the PZT-H rich surface may yield NH* (or the reverse reaction rendering ND*), NDH* or NDH_2 species and contribute to the observed isotopic exchange processes.

CONCLUSIONS

The series of experiments carried out in the present work have provided valuable information regarding the ammonia plasma synthesis and decomposition reactions and other parallel exchange processes that do not give rise to valuable products. We have proved that, plasma promoted decomposition of ammonia in a packed-bed reactor can be an energetically efficient process, provided that reaction mechanism and operating conditions are properly handled and controlled. To this end, isotopic exchange experiments using D_2 as labelling molecule have shown that besides main reaction pathways, there is panoply of intermediate hydrogen exchange reactions that consume energy but are energetically inefficient regarding the formation of either ammonia or hydrogen, depending on the desired final product. Valuable information regarding operating conditions, reactant flows, selective separation of given reactants or products, etc. can be deduced from isotope exchange experiments, thus contributing to improve reaction yields and energy efficiencies.

In addition, we have proved that the combined use of plasma diagnosis and isotopic exchange constitutes a powerful methodology to unravel plasma reaction mechanisms. In this line, we have shown that plasma-surface interaction processes directly intervene in the ammonia synthesis/decomposition reactions. We have arrived to this conclusion verifying that hydrogen incorporated in the PZT pellets may appear in the outlet gases as resulting from surface exchange processes involving intermediate N-H(D) plasma species.

Acknowledgements

We thank EU-FEDER funds and the MINECO (projects MAT2016-79866-R and CSIC 201860E050) and Junta de Andalucía (project P12-2265 MO and US-1263142) for financial support.

Supporting Information. **1.** Schematic of the reactor and experimental setup. **2.** Electrical diagnosis. **3.** Determination of the partition of labelled molecules **4.** Examples of inefficient intermediate reactions. **5.** Formation of N_2 from a plasma of NH_3+D_2. **6.** Reaction events as a function of power (ternary mixture N_2+NH_3+D_2). **7.** Evidence of the presence of excited species of deuterium in a N_2+D_2 mixture. **8.** Formation of HD and H_2 molecules during D_2 plasma activation. **9.** QMS analysis. Involvement of the PZT in the reaction processes. **10.** Estimation of the amount of H/D incorporated in the PZT pellets.

REFERENCES

(1) Kim, H.-H. Nonthermal Plasma Processing for Air-Pollution Control: A Historical Review, Current Issues, and Future Prospects. *Plasma Process. Polym.* **2004**, *1* (2), 91–110. https://doi.org/10.1002/ppap.200400028.

(2) Dobslaw, D.; Schulz, A.; Helbich, S.; Dobslaw, C.; Engesser, K.-H. VOC Removal and Odor Abatement by a Low-Cost Plasma Enhanced Biotrickling Filter Process. *J. Environ. Chem. Eng.* **2017**, *5* (6), 5501–5511. https://doi.org/10.1016/j.jece.2017.10.015.

(3) Snoeckx, R.; Bogaerts, A. Plasma Technology – a Novel Solution for CO_2 Conversion? *Chem. Soc. Rev.* **2017**, *46* (19), 5805–5863. https://doi.org/10.1039/C6CS00066E.

(4) Gómez-Ramírez, A.; M. Montoro-Damas, A.; Rodríguez, M. A.; R. González-Elipe, A.; Cotrino, J. Improving the Pollutant Removal Efficiency of Packed-Bed Plasma Reactors Incorporating Ferroelectric Components. *Chem. Eng. J.* **2017**, *314*, 311–319. https://doi.org/10.1016/j.cej.2016.11.065.

(5) Snoeckx, R.; Heijkers, S.; Van Wesenbeeck, K.; Lenaerts, S.; Bogaerts, A. CO_2 Conversion in a Dielectric Barrier Discharge Plasma: N_2 in the Mix as a Helping Hand or Problematic Impurity? *Energy Environ. Sci.* **2016**, *9* (3), 999–1011. https://doi.org/10.1039/C5EE03304G.

(6) Harris, J.; Phan, A. N.; Zhang, K. Cold Plasma Catalysis as a Novel Approach for Valorisation of Untreated Waste Glycerol. *Green Chem.* **2018**, *20* (11), 2578–2587. https://doi.org/10.1039/C8GC01163J.

(7) Montoro-Damas, A. M.; Gómez-Ramírez, A.; Gonzalez-Elipe, A. R.; Cotrino, J. Isotope Labelling to Study Molecular Fragmentation during the Dielectric Barrier Discharge Wet Reforming of Methane. *J. Power Sources* **2016**, *325*, 501–505. https://doi.org/10.1016/j.jpowsour.2016.06.028.

(8) Abd Allah, Z.; Whitehead, J. C. Plasma-Catalytic Dry Reforming of Methane in an Atmospheric Pressure AC Gliding Arc Discharge. *Catal. Today* **2015**, *256*, 76–79. https://doi.org/10.1016/j.cattod.2015.03.040.

(9) Nozaki, T.; Okazaki, K. Non-Thermal Plasma Catalysis of Methane: Principles, Energy Efficiency, and Applications. *Catal. Today* **2013**, *211*, 29–38. https://doi.org/10.1016/j.cattod.2013.04.002.

(10) Liu, J.-L.; Snoeckx, R.; Cha, M. S. Steam Reforming of Methane in a Temperature-Controlled Dielectric Barrier Discharge Reactor: The Role of Electron-Induced Chemistry

versus Thermochemistry. *J. Phys. D: Appl. Phys.* **2018**, *51* (38), 385201. https://doi.org/10.1088/1361-6463/aad7e7.

(11) Wang, L.; Yi, Y.; Guo, H.; Tu, X. Atmospheric Pressure and Room Temperature Synthesis of Methanol through Plasma-Catalytic Hydrogenation of CO2. *ACS Catal.* **2018**, *8* (1), 90–100. https://doi.org/10.1021/acscatal.7b02733.

(12) Slaets, J.; Aghaei, M.; Ceulemans, S.; Van Alphen, S.; Bogaerts, A. CO_2 and CH_4 Conversion in "Real" Gas Mixtures in a Gliding Arc Plasmatron: How Do N_2 and O_2 Affect the Performance? *Green Chem.* **2020**, *22* (4), 1366–1377. https://doi.org/10.1039/C9GC03743H.

(13) Hong, J.; Prawer, S.; Murphy, A. B. Plasma Catalysis as an Alternative Route for Ammonia Production: Status, Mechanisms, and Prospects for Progress. *ACS Sustainable Chem. Eng.* **2018**, *6* (1), 15–31. https://doi.org/10.1021/acssuschemeng.7b02381.

(14) Peng, P.; Chen, P.; Schiappacasse, C.; Zhou, N.; Anderson, E.; Chen, D.; Liu, J.; Cheng, Y.; Hatzenbeller, R.; Addy, M.; Zhang, Y.; Liu, Y.; Ruan, R. A Review on the Non-Thermal Plasma-Assisted Ammonia Synthesis Technologies. *J. Clean. Prod.* **2018**, *177*, 597–609. https://doi.org/10.1016/j.jclepro.2017.12.229.

(15) Carreon, M. L. Plasma Catalytic Ammonia Synthesis: State of the Art and Future Directions. *J. Phys. D: Appl. Phys.* **2019**, *52* (48), 483001. https://doi.org/10.1088/1361-6463/ab3b2c.

(16) Smith, C.; Hill, A. K.; Torrente-Murciano, L. Current and Future Role of Haber–Bosch Ammonia in a Carbon-Free Energy Landscape. *Energy Environ. Sci.* **2020**, *13* (2), 331–344. https://doi.org/10.1039/C9EE02873K.

(17) Gorbanev, Y.; Vervloessem, E.; Nikiforov, A.; Bogaerts, A. Nitrogen Fixation with Water Vapor by Nonequilibrium Plasma: Toward Sustainable Ammonia Production. *ACS Sustainable Chem. Eng.* **2020**, *8* (7), 2996–3004. https://doi.org/10.1021/acssuschemeng.9b07849.

(18) Hong, J.; Aramesh, M.; Shimoni, O.; Seo, D. H.; Yick, S.; Greig, A.; Charles, C.; Prawer, S.; Murphy, A. B. Plasma Catalytic Synthesis of Ammonia Using Functionalized-Carbon Coatings in an Atmospheric-Pressure Non-Equilibrium Discharge. *Plasma Chem. Plasma Process.* **2016**, *36* (4), 917–940. https://doi.org/10.1007/s11090-016-9711-8.

(19) Wang, W.; Patil, B.; Heijkers, S.; Hessel, V.; Bogaerts, A. Nitrogen Fixation by Gliding Arc Plasma: Better Insight by Chemical Kinetics Modelling. *ChemSusChem* **2017**, *10* (10), 2145–2157. https://doi.org/10.1002/cssc.201700095.

(20) Peng, P.; Chen, P.; Addy, M.; Cheng, Y.; Anderson, E.; Zhou, N.; Schiappacasse, C.; Zhang, Y.; Chen, D.; Hatzenbeller, R.; Liu, Y.; Ruan, R. Atmospheric Plasma-Assisted Ammonia Synthesis Enhanced via Synergistic Catalytic Absorption. *ACS Sustainable Chem. Eng.* **2019**, *7* (1), 100–104. https://doi.org/10.1021/acssuschemeng.8b03887.

(21) Mehta, P.; Barboun, P.; Herrera, F. A.; Kim, J.; Rumbach, P.; Go, D. B.; Hicks, J. C.; Schneider, W. F. Overcoming Ammonia Synthesis Scaling Relations with Plasma-Enabled Catalysis. *Nat. Catal.* **2018**, *1* (4), 269–275. https://doi.org/10.1038/s41929-018-0045-1.

(22) Zhu, X.; Hu, X.; Wu, X.; Cai, Y.; Zhang, H.; Tu, X. Ammonia Synthesis over $\upgamma$-Al2O3 Pellets in a Packed-Bed Dielectric Barrier Discharge Reactor. *J. Phys. D: Appl. Phys.* **2020**, *53* (16), 164002. https://doi.org/10.1088/1361-6463/ab6cd1.

(23) Sakakura, T.; Uemura, S.; Hino, M.; Kiyomatsu, S.; Takatsuji, Y.; Yamasaki, R.; Morimoto, M.; Haruyama, T. Excitation of H_2O at the Plasma/Water Interface by UV Irradiation for the Elevation of Ammonia Production. *Green Chem.* **2018**, *20* (3), 627–633. https://doi.org/10.1039/C7GC03007J.

(24) Gómez-Ramírez, A.; Cotrino, J.; Lambert, R. M.; González-Elipe, A. R. Efficient Synthesis of Ammonia from N_2 and H_2 Alone in a Ferroelectric Packed-Bed DBD Reactor. *Plasma Sources Sci. Technol.* **2015**, *24* (6), 065011. https://doi.org/10.1088/0963-0252/24/6/065011.

(25) Gómez-Ramírez, A.; Montoro-Damas, A. M.; Cotrino, J.; Lambert, R. M.; González-Elipe, A. R. About the Enhancement of Chemical Yield during the Atmospheric Plasma Synthesis of Ammonia in a Ferroelectric Packed Bed Reactor. *Plasma Process. Polym.* **2017**, *14* (6), 1600081. https://doi.org/10.1002/ppap.201600081.

(26) Akay, G.; Zhang, K. Process Intensification in Ammonia Synthesis Using Novel Coassembled Supported Microporous Catalysts Promoted by Nonthermal Plasma. *Ind. Eng. Chem. Res.* **2017**, *56* (2), 457–468. https://doi.org/10.1021/acs.iecr.6b02053.

(27) Kim, H.-H.; Teramoto, Y.; Ogata, A.; Takagi, H.; Nanba, T. Atmospheric-Pressure Nonthermal Plasma Synthesis of Ammonia over Ruthenium Catalysts. *Plasma. Process. Polym.* **2017**, *14* (6), 1600157. https://doi.org/10.1002/ppap.201600157.

(28) Peng, P.; Cheng, Y.; Hatzenbeller, R.; Addy, M.; Zhou, N.; Schiappacasse, C.; Chen, D.; Zhang, Y.; Anderson, E.; Liu, Y.; Chen, P.; Ruan, R. Ru-Based Multifunctional Mesoporous Catalyst for Low-Pressure and Non-Thermal Plasma Synthesis of Ammonia. *Int J. Hydrogen Energ.* **2017**, *42* (30), 19056–19066. https://doi.org/10.1016/j.ijhydene.2017.06.118.

(29) Patil, B. S. Plasma (Catalyst) - Assisted Nitrogen Fixation: Reactor Development for Nitric Oxide and Ammonia Production, Eindhoven University of Technology, 2017.

(30) Shah, J. R.; Gorky, F.; Lucero, J.; Carreon, M. A.; Carreon, M. L. Ammonia Synthesis via Atmospheric Plasma Catalysis: Zeolite 5A, a Case of Study. *Ind. Eng. Chem. Res.* **2020**, *59* (11), 5167–5176. https://doi.org/10.1021/acs.iecr.9b05220.

(31) Wang, Y.; Craven, M.; Yu, X.; Ding, J.; Bryant, P.; Huang, J.; Tu, X. Plasma-Enhanced Catalytic Synthesis of Ammonia over a Ni/Al2O3 Catalyst at Near-Room Temperature: Insights into the Importance of the Catalyst Surface on the Reaction Mechanism. *ACS Catal.* **2019**, *9* (12), 10780–10793. https://doi.org/10.1021/acscatal.9b02538.

(32) Shah, J.; Wang, W.; Bogaerts, A.; Carreon, M. L. Ammonia Synthesis by Radio Frequency Plasma Catalysis: Revealing the Underlying Mechanisms. *ACS Appl. Energy Mater.* **2018**, *1* (9), 4824–4839. https://doi.org/10.1021/acsaem.8b00898.

(33) Yaala, M. B.; Saeedi, A.; Scherrer, D.-F.; Moser, L.; Steiner, R.; Zutter, M.; Oberkofler, M.; Temmerman, G. D.; Marot, L.; Meyer, E. Plasma-Assisted Catalytic Formation of Ammonia in N2–H2 Plasma on a Tungsten Surface. *Phys. Chem. Chem. Phys.* **2019**, *21* (30), 16623–16633. https://doi.org/10.1039/C9CP01139K.

(34) Shah, J.; Gorky, F.; Psarras, P.; Seong, B.; Gómez-Gualdrón, D. A.; Carreon, M. L. Enhancement of the Yield of Ammonia by Hydrogen-Sink Effect during Plasma Catalysis. *ChemCatChem* **2020**, *12* (4), 1200–1211. https://doi.org/10.1002/cctc.201901769.

(35) Navascués, P.; Obrero-Pérez, J. M.; Cotrino, J.; González-Elipe, A. R.; Gómez-Ramírez, A. Isotope Labelling for Reaction Mechanism Analysis in DBD Plasma Processes. *Catalysts* **2019**, *9* (1), 45. https://doi.org/10.3390/catal9010045.

(36) Barboun, P.; Mehta, P.; Herrera, F. A.; Go, D. B.; Schneider, W. F.; Hicks, J. C. Distinguishing Plasma Contributions to Catalyst Performance in Plasma-Assisted Ammonia Synthesis. *ACS Sustainable Chem. Eng.* **2019**, *7* (9), 8621–8630. https://doi.org/10.1021/acssuschemeng.9b00406.

(37) Peng, P.; Li, Y.; Cheng, Y.; Deng, S.; Chen, P.; Ruan, R. Atmospheric Pressure Ammonia Synthesis Using Non-Thermal Plasma Assisted Catalysis. *Plasma Chem. Plasma Process.* **2016**, *36* (5), 1201–1210. https://doi.org/10.1007/s11090-016-9713-6.

(38) Peng, P.; Chen, P.; Addy, M.; Cheng, Y.; Zhang, Y.; Anderson, E.; Zhou, N.; Schiappacasse, C.; Hatzenbeller, R.; Fan, L.; Liu, S.; Chen, D.; Liu, J.; Liu, Y.; Ruan, R. In Situ Plasma-Assisted Atmospheric Nitrogen Fixation Using Water and Spray-Type Jet Plasma. *Chem. Commun.* **2018**, *54* (23), 2886–2889. https://doi.org/10.1039/C8CC00697K.

(39) Shah, J. R. Non-Thermal Plasma Catalytic Synthesis of Ammonia, University of Tulsa, 2019.

(40) Hayakawa, Y.; Miura, T.; Shizuya, K.; Wakazono, S.; Tokunaga, K.; Kambara, S. Hydrogen Production System Combined with a Catalytic Reactor and a Plasma Membrane Reactor from Ammonia. *Int. J. Hydrogen Energ.* **2019**, *44* (20), 9987–9993. https://doi.org/10.1016/j.ijhydene.2018.12.141.

(41) Yi, Y.; Wang, L.; Guo, Y.; Sun, S.; Guo, H. Plasma-Assisted Ammonia Decomposition over Fe–Ni Alloy Catalysts for CO_x - Free Hydrogen. *AIChE J.* **2018**, aic.16479. https://doi.org/10.1002/aic.16479.

(42) Yi, Y.; Wang, L.; Hongchen, G. Plasma-Catalytic Decomposition of Ammonia for Hydrogen Energy. In *Plasma Catalysis: Fundamentals and Applications*; Tu, X., Whitehead, C., Nozaki, T., Eds.; Springer Series on Atomic, Optical and Plasma Physics; Springer: Switzerland, 2019; Vol. 106, pp 181–231.

(43) Daou, F.; Vincent, A.; Amouroux, J. Point and Multipoint to Plane Barrier Discharge Process for Removal of NOx from Engine Exhaust Gases: Understanding of the Reactional Mechanism by Isotopic Labeling. *Plasma Chem. Plasma Process.* **2003**, *23* (2), 309–325. https://doi.org/10.1023/A:1022972103224.

(44) Peeters, F.; Butterworth, T. Electrical Diagnostics of Dielectric Barrier Discharges. In *Atmospheric Pressure Plasma: from Diagnostics to Applications*; Nikiforov, A., Chen, Z., Eds.; Plasma Physics; IntechOpen: England, 2019; pp 1–27.

(45) Montoro-Damas, A. M.; Brey, J. J.; Rodríguez, M. A.; González-Elipe, A. R.; Cotrino, J. Plasma Reforming of Methane in a Tunable Ferroelectric Packed-Bed Dielectric Barrier Discharge Reactor. *J. Power Sources* **2015**, *296*, 268–275. https://doi.org/10.1016/j.jpowsour.2015.07.038.

(46) Kim, Y.-K.; Irikura, K. K.; Rudd, M. E.; Ali, M. A.; Stone, P. M.; Chang, J.; Coursey, J. S.; Dragoset, R. A.; Kishore, A. R.; Olsen, K. J.; Sansonetti, A. M.; Wiersma, G. G.; Zucker, D. S.; Zucker, M. A. Electron-Impact Cross Sections for Ionization and Excitation Database. In *NIST Standard Reference Database*; USA, 2004; Vol. 107.

(47) Yun, S.; Ted Oyama, S. Correlations in Palladium Membranes for Hydrogen Separation: A Review. *J. Membrane Sci.* **2011**, *375* (1–2), 28–45. https://doi.org/10.1016/j.memsci.2011.03.057.

(48) Pearse, R. W. B.; Gaydon, A. G. *The Identification of Molecular Spectra*, 3rd ed.; Chapman and Hall Ltd.: England, 1965.

(49) Stapelmann, K.; Lackmann, J.-W.; Buerger, I.; Bandow, J. E.; Awakowicz, P. A H $_2$ Very High Frequency Capacitively Coupled Plasma Inactivates Glyceraldehyde 3-Phosphate Dehydrogenase (GapDH) More Efficiently than UV Photons and Heat Combined. *J. Phys. D: Appl. Phys.* **2014**, *47* (8), 085402. https://doi.org/10.1088/0022-3727/47/8/085402.

(50) Shah, J. R.; Harrison, J. M.; Carreon, M. L. Ammonia Plasma-Catalytic Synthesis Using Low Melting Point Alloys. *Catalysts* **2018**, *8* (10), 437. https://doi.org/10.3390/catal8100437.

(51) van den Oever, P. J.; van Helden, J. H.; Lamers, C. C. H.; Engeln, R.; Schram, D. C.; van de Sanden, M. C. M.; Kessels, W. M. M. Density and Production of NH and NH2 in an Ar–NH3 Expanding Plasma Jet. *J. Appl. Phys.* **2005**, *98* (9), 093301. https://doi.org/10.1063/1.2123371.

(52) Yin, K. S.; Venugopalan, M. Plasma Chemical Synthesis. I. Effect of Electrode Material on the Synthesis of Ammonia. *Plasma Chem. Plasma Process.* **1983**, *3* (3), 343–350. https://doi.org/10.1007/BF00564632.

(53) Bogaerts, A.; Zhang, Q.-Z.; Zhang, Y.-R.; Van Laer, K.; Wang, W. Burning Questions of Plasma Catalysis: Answers by Modeling. *Catal. Today* **2019**, *337*, 3–14. https://doi.org/10.1016/j.cattod.2019.04.077.

(54) Rouwenhorst, K. H. R.; Kim, H.-H.; Lefferts, L. Vibrationally Excited Activation of N $_2$ in Plasma-Enhanced Catalytic Ammonia Synthesis: A Kinetic Analysis. *ACS Sustainable Chem. Eng.* **2019**, *7* (20), 17515–17522. https://doi.org/10.1021/acssuschemeng.9b04997.

(55) Snels, M.; Fusina, L.; Hollenstein, H.; Quack, M. The v 1 and v 3 Bands of ND3. *Mol. Phys.* **2000**, *98* (13), 837–854. https://doi.org/10.1080/00268970050025457.

(56) Snels, M.; Hollenstein, H.; Quack, M. The NH and ND Stretching Fundamentals of 14ND2H. *J. Chem. Phys.* **2003**, *119* (15), 7893–7902. https://doi.org/10.1063/1.1592506.

(57) Shimanouchi, T. Tables of Molecular Vibrational Frequencies. In *NIST Standard Reference Database*; USA, 1972; Vol. 1.

(58) Huang, C.-K.; Wu, T.-B. Plasma Etching and Hydrogen Blocking Characteristics of PtOx Thin Films in Ferroelectric Capacitor Fabrication. *Appl. Phys. Lett.* **2003**, *83* (15), 3147–3149. https://doi.org/10.1063/1.1610250.

(59) Drogowska, K.; Flege, S.; Rogalla, D.; Becker, H.-W.; Ionescu, E.; Kim-Ngan, N.-T. H.; Balogh, A. G. Hydrogen Content Analysis in Hydrogen-Charged PZT Ferroelectric Ceramics. *Solid State Ionics* **2013**, *235*, 32–35. https://doi.org/10.1016/j.ssi.2013.01.009.

(60) Mohammadabadi, A. S. Hydrogen-induced Damage of Lead-zirconate-titanate (PZT), University of British Columbia, 2013. https://doi.org/10.14288/1.0073678.

(61) Liyanage, M.; Miller, R.; Rajapakse, R. First Principles Study of Hydrogen in Lead Zirconate Titanate. *Smart Mater. Struct.* **2019**, *28* (3), 034002. https://doi.org/10.1088/1361-665X/aafeed.

TABLE OF CONTENTS

Isotope labelling identification of discharge and surface reaction mechanisms lessening the efficiencies of plasma-driven hydrogen or ammonia synthesis